Int. J. Solids Structures Vol. 30, No. 3, pp. 441–452, 1993
Printed in Great Britain.

0020-7683/93 $5.00+ .00
© 1992 Pergamon Press Ltd

A REFINED FINITE STRIP METHOD USING HIGHER-ORDER PLATE THEORY

Y.-P. TSENG and W. J. WANG
Department of Civil Engineering, Tamkang University, Taiwan 25137, R.O.C.

(*Received* 13 *May* 1991; *in revised form* 15 *July* 1992)

Abstract—The higher-order plate theory is adopted in the finite strip method to analyse orthotropic laminated plates in this paper. Several examples with the existing elasticity solutions are illustrated to validate the accuracy and efficiency of the present formulation. Although fewer degrees of freedom are required, the present model yields the same or even better displacement and flexural stress results than the higher-order plate element. The through-thickness distribution of transverse shear stress is also properly predicted through the stress equilibrium equation.

INTRODUCTION

The classical plate theory, which ignores transverse shear effects, can provide reasonable predictions only for relatively thin plates. To take account of the effects of transverse shear deformation, a number of improved "thick" plate theories have been developed. One of these is the Mindlin plate theory in which a straight line originally normal to the plate median surface will be straight but not normal after deformation. Recently, several C^0 higher-order plate theories have been developed by Lo *et al.* (1977), Levinson (1980) and Kant and Pandya (1988) to consider transverse shear effects and the warping of the cross-section. Therefore, the straight line becomes curved after deformation. The transverse normal stress is further considered in the displacement model by Lo *et al.* Reddy (1984a) proposed a refined C^1 higher-order plate theory satisfying the zero transverse shear stress conditions on the plate top and bottom surfaces.

The finite strip method has been considered to be a more efficient computational tool than the finite element method for the prismatic structure. However, the transverse shear deformations are neglected in the classical plate theory used by Cheung and Cheung (1972). As an attempt to include the transverse shear effects, Mawenya and Davies (1974) applied the finite strip method to the Mindlin plate theory. Therefore, it is good for thin and moderately thick plates. Later, the X-spline finite strip method proposed by Yang and Chong (1984) was also explored to allow for the nonprismatic structures to be analysed. It is surprising that the combination of higher-order plate theory with the finite strip method was not found in the literature.

The present study serves as a preliminary study on the application of the higher-order plate theory to the finite strip method in the analysis of laminated plates. The assumed displacement model by Lo *et al.* is adopted, and the C^0 approach is attractive due to the simplicity and implementation in programming. Through several comparative examples, it has been revealed that the accuracy of the present model is comparable to the closed-form and other finite element solutions. The through-thickness distribution of transverse shear stresses was also evaluated through the stress equilibrium equation, and good agreement with the elasticity solution was observed.

FINITE STRIP FORMULATION

The displacement field of higher-order plate theory assumed by Lo *et al.* (1977) is adopted. Thus,

$$\begin{aligned} u(x,y,z) &= u_0(x,y)+z\theta_y(x,y)+z^2u^*(x,y)+z^3\theta_y^*(x,y),\\ v(x,y,z) &= v_0(x,y)+z\theta_x(x,y)+z^2v^*(x,y)+z^3\theta_x^*(x,y),\\ w(x,y,z) &= w_0(x,y)+z\theta_z(x,y)+z^2w^*(x,y). \end{aligned} \tag{1}$$

The above displacement assumption is written in matrix form as

$$\{\Delta\} = [L]\{d\}, \tag{2}$$

where z is the distance from the panel midplane, $\{\Delta\} = \{u, v, w\}$ is the 3-D displacement field, and $\{d\} = \{u_0, v_0, w_0, \theta_x, \theta_y, \theta_z, u^*, v^*, w^*, \theta_x^*, \theta_y^*\}$ is the midplane displacement field including 11 variables, as shown in Fig. 1.

Since the C^0-continuous displacement model is adopted, the midplane displacement $\{d\}$ for a typical strip is interpolated by nodal displacements $\{q\}$ as

$$\{d\} = [N]\{q\} = \sum_{i=1}^{nst} [N_i]\{q_i\}, \tag{3}$$

where nst is the nodal number per strip, $[N]\backslash[N_i]$ are the matrices of shape functions, and $\{q_i\} = \{u_{0i}, v_{0i}, w_{0i}, \theta_{xi}, \theta_{yi}, \theta_{zi}, u_i^*, v_i^*, w_i^*, \theta_{xi}^*, \theta_{yi}^*\}$ are nodal displacements.

In the semi-analytical finite strip method, the simple polynominals are used in the transverse direction and the continuous eigenfunctions are in the longitudinal direction, with the latter satisfying *a priori* the end boundary conditions of the strip. The eigenfunction $Y_m(y)$ for various end conditions can be found in Cheung (1976). For a strip with both $y = 0$ and $y = b$ ends simply supported,

$$Y_m(y) = \sin(m\pi y/b), \quad m = 1, 2, 3, \ldots \tag{4}$$

As the 3-noded strip element is adopted, the shape functions $N_i(\xi)$ the same as the usual finite element method are

$$N_i(\xi) = -\xi(1-\xi)/2, 1-\xi^2, \xi(1+\xi)/2, \quad i = 1, 2, 3. \tag{5}$$

The interpolation of midplane displacements can be written explicitly as

$$\begin{aligned}
u_0 &= \sum_{i=1}^{nst}\sum_{m=1}^{r} Y_m(y)N_i(x)u_0^i, & v_0 &= \sum_{i=1}^{nst}\sum_{m=1}^{r} Y'_m(y)N_i(x)v_0^i,\\
w_0 &= \sum_{i=1}^{nst}\sum_{m=1}^{r} Y_m(y)N_i(x)w_0^i, & \theta_x &= \sum_{i=1}^{nst}\sum_{m=1}^{r} Y'_m(y)N_i(x)\theta_x^i,\\
\theta_y &= \sum_{i=1}^{nst}\sum_{m=1}^{r} Y_m(y)N_i(x)\theta_y^i, & \theta_z &= \sum_{i=1}^{nst}\sum_{m=1}^{r} Y_m(y)N_i(x)\theta_z^i,\\
u^* &= \sum_{i=1}^{nst}\sum_{m=1}^{r} Y_m(y)N_i(x)u^{*i}, & v^* &= \sum_{i=1}^{nst}\sum_{m=1}^{r} Y'_m(y)N_i(x)v^{*i},\\
w^* &= \sum_{i=1}^{nst}\sum_{m=1}^{r} Y_m(y)N_i(x)w^{*i}, & \theta_x^* &= \sum_{i=1}^{nst}\sum_{m=1}^{r} Y'_m(y)N_i(x)\theta_x^{*i},\\
\theta_y^* &= \sum_{i=1}^{nst}\sum_{m=1}^{r} Y_m(y)N_i(x)\theta_y^{*i},
\end{aligned} \tag{6}$$

where r is the number of terms used in the series of eigenfunctions.

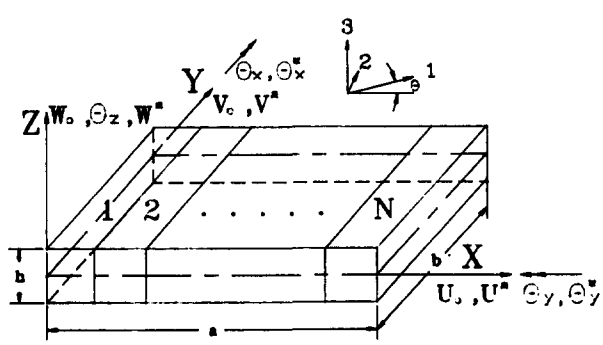

Fig. 1. Geometry of strips and laminated plates.

The 3-D displacement $\{\Delta\}$ is also obtained by substituting (3) into (2) to obtain

$$\{\Delta\} = [\bar{N}]\{q\} = \sum_{i=1}^{nst} \sum_{m=1}^{r} [L][N_i] Y_m(y)\{q_i\}, \tag{7}$$

where $[\bar{N}]$ is the shape function matrix.

Based on the small deformation theory, the strains are constructed as

$$\begin{aligned}
\varepsilon_x &= u_{,x} = u_{0,x} + z\theta_{y,x} + z^2 u^*_{,x} + z^3\theta^*_{y,x},\\
\varepsilon_y &= v_{,y} = v_{0,y} + z\theta_{x,y} + z^2 v^*_{,y} + z^3\theta^*_{x,y},\\
\varepsilon_z &= w_{,z} = \theta_{z,z} + 2zw^*_{,z},\\
\gamma_{xy} &= u_{,y} + v_{,x}\\
&= (u_{0,y} + v_{0,x}) + z(\theta_{y,y} + \theta_{x,x}) + z^2(u^*_{,y} + v^*_{,x}) + z^3(\theta^*_{x,x} + \theta^*_{y,y}),\\
\gamma_{xz} &= u_{,z} + w_{,x} = w_{0,x} + z\theta_{z,x} + z^2 w^*_{,x} + \theta_y + 2zu^* + 3z^2\theta^*_y,\\
\gamma_{yz} &= v_{,z} + w_{,y} = w_{0,y} + z\theta_{z,x} + z^2 w^*_{,y} + \theta_x + 2zv^* + 3z^2\theta^*_x.
\end{aligned} \tag{8}$$

The generalized midplane strain is therefore defined as

$$\begin{aligned}
\{\bar{\varepsilon}\} = \{\{&u_{0,x}; v_{0,y}; u_{0,y} + v_{0,x}; \theta_z; u^*_{,x}; v^*_{,y}; u^*_{,y} + v^*_{,x}\}, \{\theta_{x,y}; \theta_{y,x};\\
&\theta_{y,y} + \theta_{x,x}; 2w^*; \theta^*_{x,y}; \theta^*_{y,x}; \theta^*_{x,x} + \theta^*_{y,y}\}, \{w_{0,x} + \theta_y; w_{0,y} + \theta_x;\\
&2u^* + \theta_{z,y}; 2v^* + \theta_{z,x}; w_{0,x} + 3\theta^*_y; w_{0,y} + 3\theta^*_x\}\}.
\end{aligned} \tag{9}$$

With the above definitions, $\{\bar{\varepsilon}\}$ is related to $\{d\}$ by

$$\{\bar{\varepsilon}\} = [\bar{B}]\{d\}, \tag{10}$$

where $[\bar{B}]$ is the proper differential operating matrix.

Correspondingly, the midplane stress resultants are defined as

$$\begin{aligned}
\{\bar{\sigma}\} = \{\{&N_x, N_y, N_{xy}, N^*_x, N^*_y, N^*_{xy}, N_z\}, \{M_x, M_y, M_{xy},\\
&M^*_x, M^*_y, M^*_{xy}, M_z\}, \{Q_x, Q_y, S_x, S_y, Q^*_x, Q^*_y\}\}
\end{aligned}$$

$$\begin{pmatrix} N_x & N_y & N_{xy} & N_z \\ M_x & M_y & M_{xy} & M_z \end{pmatrix} = \sum_{k=1}^{n^1} \int_{h_k}^{h_{k+1}} \begin{Bmatrix} 1 \\ z \end{Bmatrix} [\sigma^k_x \sigma^k_y \tau^k_{xy} \sigma^k_z]\, \mathrm{d}z,$$

$$\begin{pmatrix} N^*_x & N^*_y & N^*_{xy} \\ M^*_x & M^*_y & M^*_{xy} \end{pmatrix} = \sum_{k=1}^{n1} \int_{h_k}^{h_{k+1}} \begin{Bmatrix} z^2 \\ z^3 \end{Bmatrix} [\sigma^k_x\, \sigma^k_y\, \tau^k_{xy}]\, \mathrm{d}z,$$

$$\begin{pmatrix} Q & Q_y \\ S_x & S_y \\ Q^*_x & Q^*_y \end{pmatrix} = \sum_{k=1}^{n^1} \int_{h_k}^{h_{k+1}} \begin{Bmatrix} 1 \\ z \\ z^2 \end{Bmatrix} [\tau^k_{xz}\ \ \tau^k_{yz}]\, \mathrm{d}z \tag{11}$$

(nl is the total number of layers and h_i is the vectorial distance from the panel midplane).

The constitutive equation is then the relation

$$\{\bar{\sigma}\} = [D]\{\bar{\varepsilon}\} = [D][\bar{B}]\{d\}, \tag{12}$$

where the material property matrix $[D]$ is the same as that used in Lo *et al.* (1977).

The laminated plate is divided into n strips and each strip accumulates nl layers. The total potential energy π of the strip element is therefore given by the following equation:

$$\pi = \sum_{i=1}^{n} \sum_{k=1}^{n1} \left(\frac{1}{2} \int_{v_{ni}} (\{\varepsilon\}^t \{\sigma^k\})\, \mathrm{d}V - \int_{S\sigma_{ni}} \{\Delta\}^t \{\bar{T}\}\, \mathrm{d}S \right), \tag{13}$$

where $\{\varepsilon\}$ is the strain, $\{\sigma\}$ is the stress, V_{ni} is the volume of the ith strip, $\{\bar{T}\}$ is the transverse loading, and $S\sigma_{ni}$ is the area in the ith strip subjected to transverse loading.

Integrating π through the thickness, the stresses $\{\sigma\}$ become the midplane stress resultants $\{\bar{\sigma}\}$, and the strains $\{\varepsilon\}$ are then replaced with the midplane strains $\{\bar{\varepsilon}\}$. Thus, the functional π becomes

$$\pi = \sum_{i=1}^{n} \left[\frac{1}{2} \int_{R_{ni}} (\{\bar{\varepsilon}\}^t \{\bar{\sigma}\}) \, \mathrm{d}A - \int_{S\sigma_{ni}} \{\Delta\}^t \{\bar{T}\} \, \mathrm{d}S \right), \tag{14}$$

where R_{ni} is the midplane area of the ith strip.

By substituting (10) and (12) into the last equation, the total potential energy is expressed as

$$\pi = \sum_{i=1}^{n} \frac{1}{2} \int_{R_{ni}} ([\bar{B}]\{d\})^t [D][\bar{B}]\{d\} \, \mathrm{d}A - \int_{S\sigma_{ni}} \{\Delta\}^t \{\bar{T}\} \, \mathrm{d}S. \tag{15}$$

In finite strip formulation, the midplane displacements $\{d\}$ and the 3-D displacements $\{\Delta\}$ are both interpolated by nodal displacement $\{q\}$. Substitution of (3) and (16) into (15) yields

$$\pi = \sum_{i=1}^{n} \frac{1}{2} \{q\}^t \int_{R_{ni}} [B]^t [D][B] \, \mathrm{d}A \, \{q\} - \sum_{i=1}^{n} \int_{S\sigma n_i} \{q\}^t [\bar{N}]^t \{\bar{T}\} \, \mathrm{d}S, \tag{16}$$

where $[B]$ is the strain–displacement matrix.

This leads to the stiffness matrix and loading vector,

$$[k] = \int_{R_{ni}} [B]^t [D] [B] \, \mathrm{d}A, \quad \{Q\} = \int_{S\sigma_{ni}} [\bar{N}]^t \{\bar{T}\} \, \mathrm{d}S. \tag{17}$$

The equation for a plate strip element is derived as

$$[k] \{q\} = \{Q\}. \tag{18}$$

Assembling (18), the finite strip equation becomes

$$[K] \{r\} = \{R\}, \tag{19}$$

where $[K]$, $\{r\}$, $\{R\}$ are global stiffness, displacement and loading, respectively.

Based on the attained values for $\{r\}$ and height z, the displacement analysis of any point is accomplished. Flexural stresses are computed from the constitutive relation. However, the through-thickness distribution of transverse shear stresses is calculated from flexural stresses through the stress equilibrium equation in this paper.

NUMERICAL EXAMPLES

The performance of the present refined finite strip method associated with the higher-order plate theory is demonstrated through several benchmark problems. So that they can be compared with the existing closed-form solutions, the edges of rectangular plates are considered to be invariably simply supported and the transverse loading is assumed to be sinusoidally or uniformly distributed. It is also assumed that the material and thickness for all layers are the same. The orthotropic material properties on principle axes are

$$E_{11} = 25 \times 10^6 \,\text{psi}, \quad E_{22} = E_{33} = 1 \times 10^6 \,\text{psi}, \quad G_{12} = G_{13} = 0.5 \times 10^6 \,\text{psi},$$
$$G_{23} = 0.2 \times 10^6 \,\text{psi}, \quad \nu_{12} = \nu_{23} = \nu_{13} = 0.25.$$

For the purpose of comparison, the following normalized quantities are employed:

$$\bar{w} = \frac{100E_{22}w}{q_0hS^4}, \quad \bar{u} = \frac{E_{22}u}{q_0hS^3},$$

$$(\bar{\sigma}_x, \bar{\sigma}_y, \bar{\tau}_{xy}) = \frac{1}{q_0h^3S^2}(\sigma_x, \sigma_y, \tau_{xy}),$$

$$(\bar{\tau}_{xz}, \bar{\tau}_{yz}, \bar{\sigma}_z) = \frac{1}{q_0S}(\tau_{xz}, \tau_{yz}, \sigma_z),$$

$$\text{Error}\,\% = \frac{\bar{w}(\text{FEM}) - \bar{w}(\text{Elasticity Solution})}{\bar{w}\,(\text{Elasticity Solution})}\,\%,$$

where $S = a/h$ is the span-to-thickness ratio.

The numerical results obtained by the present finite strip method are represented by FSM, and the results of the higher order plate element by Kant and Pandya (1988) are indicated as HOPE. Since fast convergence is shown below, a full plate of 10 strips is modelled, unless stated otherwise. The transverse deflection $\bar{w}$, flexural stresses σ_x, σ_y, τ_{xy} at the centre of the plate, and transverse shear stresses τ_{xz} at $(0, b/2)$, and τ_{yz} at $(a/2, 0)$ are particularly interested since they are of the maximum values.

Single-layer plate

A simply-supported square plate is subjected to a sinusoidal transverse loading $q_0 \sin(\pi x/a) \sin(\pi y/b)$. The value of q_0 is arbitrary since dimensionless quantities are used. One term of the eigenfunction series is used since there is only one term in this loading. The normalized centre deflections for plates of span-to-thickness ratios 4–100 are tabulated in Table 1. The elasticity solution by Pagano (1969) and the Navier's solution in Reddy's book (1984b) are also appended for comparison. Excellent accuracy is observed. The error for the $S = 4$ plate is restricted to only 0.06%.

Two-layer composite laminate

This example is to illustrate the effect of mesh refinement on the deflection and stress predictions in the present development. Two-layer cross-ply (0°/90°) square laminated plates are simply-supported along the edges and are subjected to sinusoidal loading.

The convergence studies of normalized centre transverse deflection and flexural stresses for thick ($S = 4$), moderately thick ($S = 10$), and thin ($S = 50$) laminates are tabulated in Tables 2–4, respectively. The plate is divided into 2, 4, 6 and 10 strips. Compared to Pagano's elasticity solution, the present FSM results are all better than those of HOPE. This improvement is more evident in thick plates. In the analysis of the $S = 10$ moderately thick plate, the error of 1.56% by HOPE is reduced to 1.18% for FSM. For the $S = 4$ plate, the error of 5.7% is reduced to 2.40%. The flexural stresses are secondary variables and then there exist slightly larger deviations. However, the present results are better than

Table 1. Normalized transverse maximum deflection of single square plate

Deflection $\bar{w} = 100E_{22}w(a/2, b/2, 0)/q_0hS^4$			
	Present	Navier	Pagano
$S = 4$	1.60729	0.42612	1.60827
$S = 10$	0.63693	0.42612	0.63913
$S = 20$	0.48357	0.42612	0.48647
$S = 50$	0.43966	0.42612	0.44275
$S = 100$	0.43335	0.42612	0.43647

Navier (1984b): closed-form solution of the classical plate theory.
Pagano (1969): elasticity solution.

Table 2. Normalized stresses and deflection of two-layer, (0°/90°) square plate. $S = 4$

Source (mesh)	$\bar{\sigma}_x$	$\bar{\tau}_{xy}$	$\bar{\tau}_{xz}$	$\bar{w}$
Present 2	0.7492 −0.1126	−0.05882 0.05693	0.1029	2.0303
Present 4	0.7817 −0.1119	−0.05857 0.05764	0.1241	2.0253
Present 6	0.7763 −0.1113	−0.05832 0.05784	0.1283	2.0250
Present 10	0.7730 −0.1110	−0.05816 0.05790	0.1304	2.0249
Pagano	0.7807 −0.1098	−0.05910 0.05880	0.1353	2.0741
Kant *et al.* 2×2	1.0181 −0.0926	−0.06000 0.06000	0.0954	1.9563

Kant *et al.* (1988): higher-order plate element
locations: $\bar{\sigma}_x$ at $(a/2, a/2, \pm 0.5)$, $\bar{\tau}_{xy}$ at $(0, 0, \pm 0.5)$, $\bar{\tau}_{xz}$ at $(0, a/2, 0)$, $\bar{w}$ at $(a/2, a/2, 0)$.

Table 3. Normalized stresses and deflection of two-layer, (0°/90°) square plate. $S = 10$

Source (mesh)	$\bar{\sigma}_x$	$\bar{\tau}_{xy}$	$\bar{\tau}_{xz}$	$\bar{w}$
Present 2	0.7518 −0.9109	−0.05413 0.05693	0.1018	1.2233
Present 4	0.7383 −0.8993	−0.05399 0.05320	0.1179	1.2205
Present 6	0.7331 −0.8938	−0.05376 0.05330	0.1212	1.2202
Present 10	0.7300 −0.8905	−0.05361 0.05334	0.1228	1.2202
Pagano	0.7300 −0.0890	−0.05380 0.05360	0.1250	1.2320
Kant *et al.* 2×2	0.7593 −0.0855	−0.05370 0.05370	0.1086	1.2128

Table 4. Normalized stresses and deflection of two-layer, (0°/90°) square plate. $S = 50$

Source (mesh)	$\bar{\sigma}_x$	$\bar{\tau}_{xy}$	$\bar{\tau}_{xz}$	$\bar{w}$
Present 2	0.7403 −0.0872	−0.0534 0.0521	0.1023	1.0722
Present 4	0.7266 −0.0858	−0.0530 0.0525	0.1167	1.0701
Present 6	0.7213 −0.0852	−0.0528 0.0525	0.1196	1.0699
Present 10	0.7300 −0.8905	−0.0536 0.0533	0.1211	1.0698
Pagano	0.7235 −0.0846	−0.0528 0.0526	0.1216	1.0744
Kant *et al.* 2×2	0.7244 −0.0852	−0.0537 0.0530	0.1086	1.2128

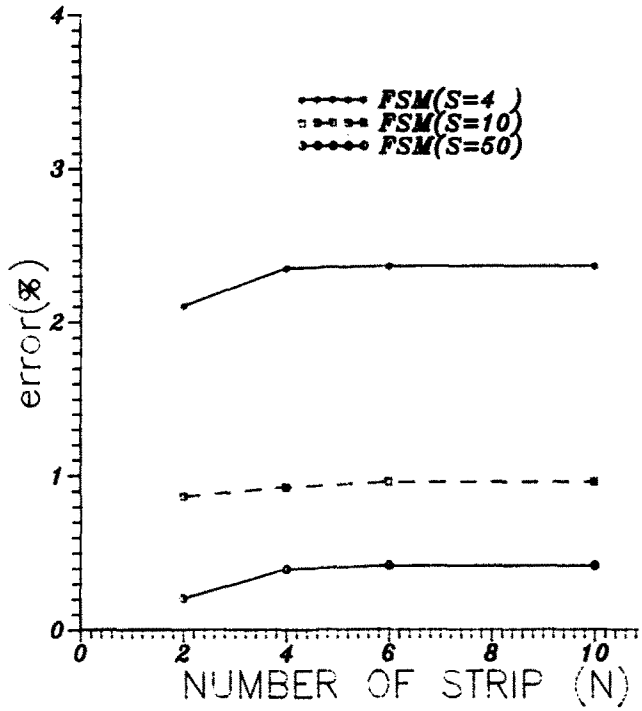

Fig. 2. Number of strips for convergence of centre deflection.

the results of HOPE. Note that the convergence is quite rapid. Further illustrations for the convergence of centre deflection are shown in Fig. 2. The effects of the span-to-thickness ratio on the accuracy of maximum deflections is also exhibited in Fig. 3.

Figure 4 shows the variation of in-plane deformation $\bar{u}$ through the thickness of the laminate for the $S = 4$ thick plate. Both FSM and HOPE are close to the elasticity solution. The unusual distortion of the cross-section is also closely predicted herein.

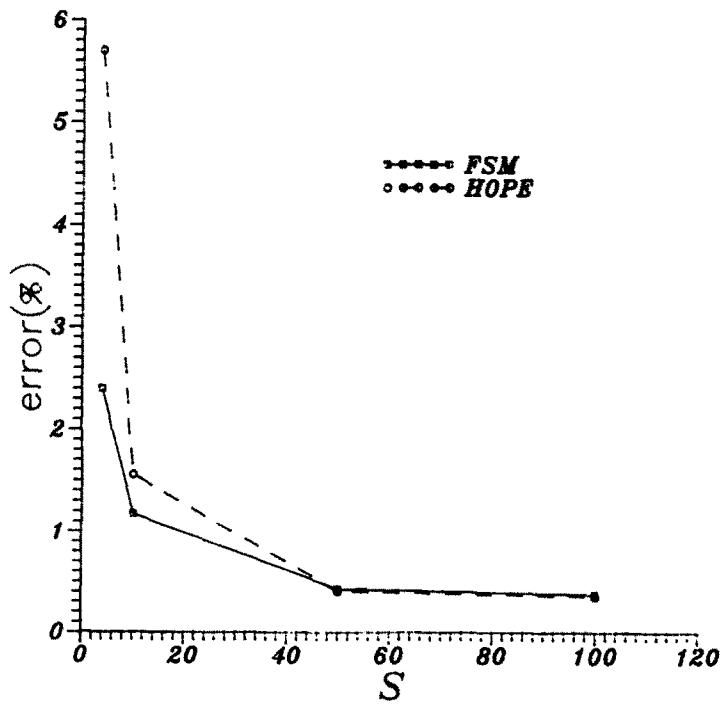

Fig. 3. Effect of span-to-thickness ratio on the accuracy of maximum central displacement.

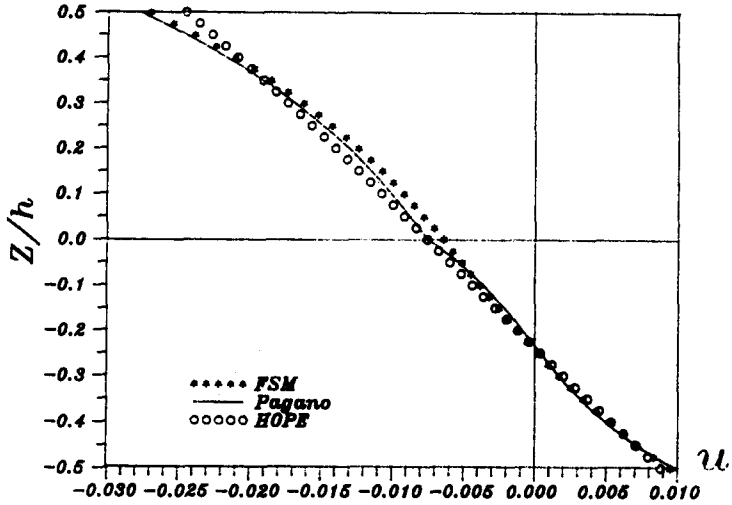

Fig. 4. Through-thickness distribution of in-plane deformation $\bar{u}(a/2, a/2, z/h)$ for $a/h = 4$ two-layered plate.

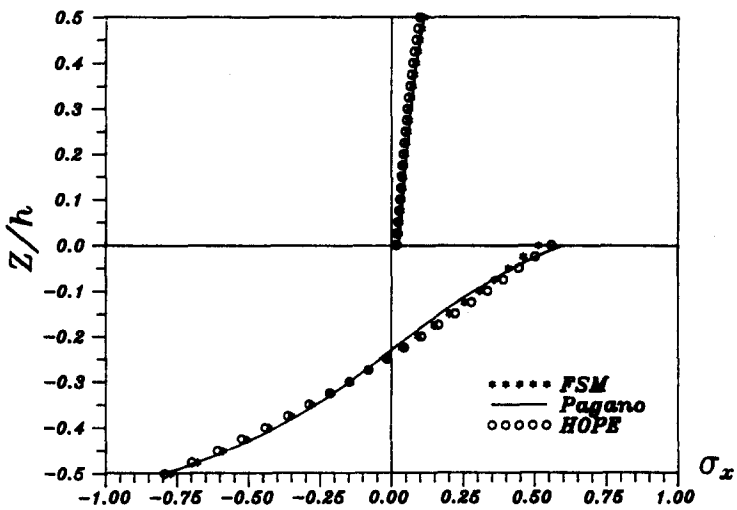

Fig. 5. Through-thickness distribution of in-plane stress $\bar{\sigma}_x(a/2, a/2, z/h)$ for $a/h = 4$ two-layered plate.

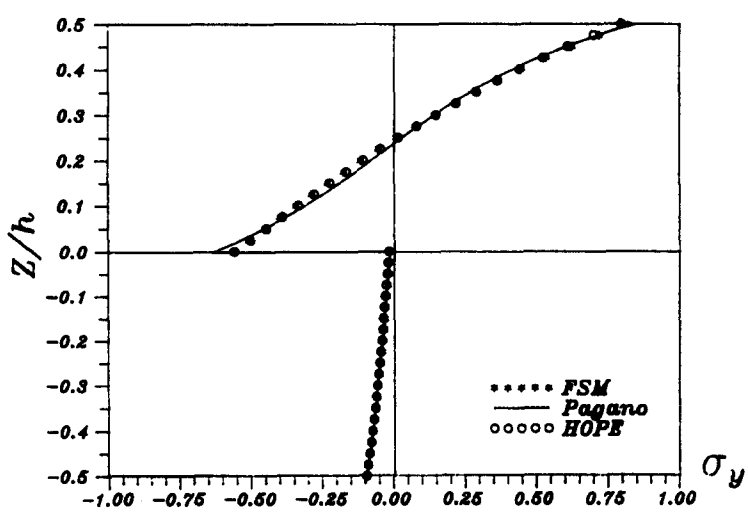

Fig. 6. Through-thickness distribution of in-plane stress $\bar{\sigma}_y(a/2, a/2, z/h)$ for $a/h = 4$ two-layered plate.

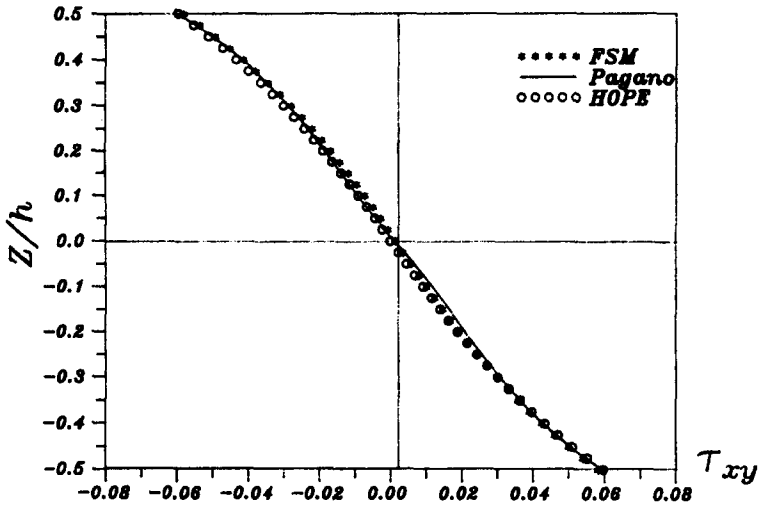

Fig. 7. Through-thickness distribution of in-plane stress $\bar{\tau}_{xy}(0, 0, z/h)$ *for* $a/h = 4$ two-layered plate.

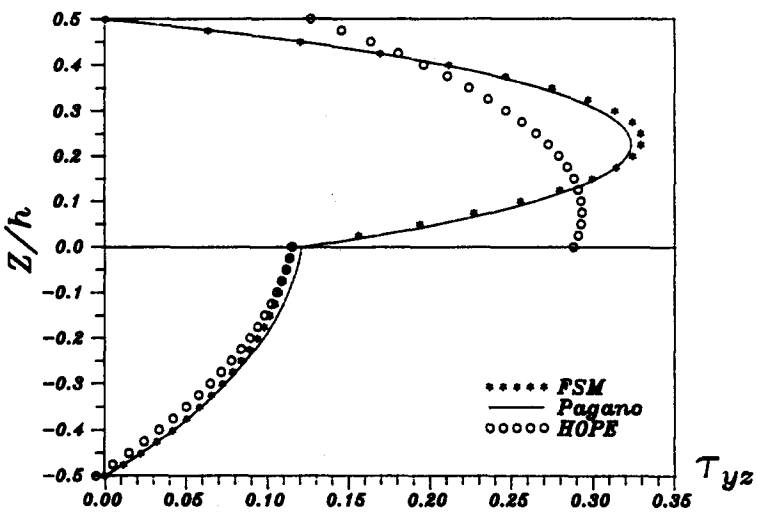

Fig. 8. Through-thickness distribution of transverse shear stress $\bar{\tau}_{yz}(a/2, 0, z/h)$ for $a/h = 4$ two-layered plate.

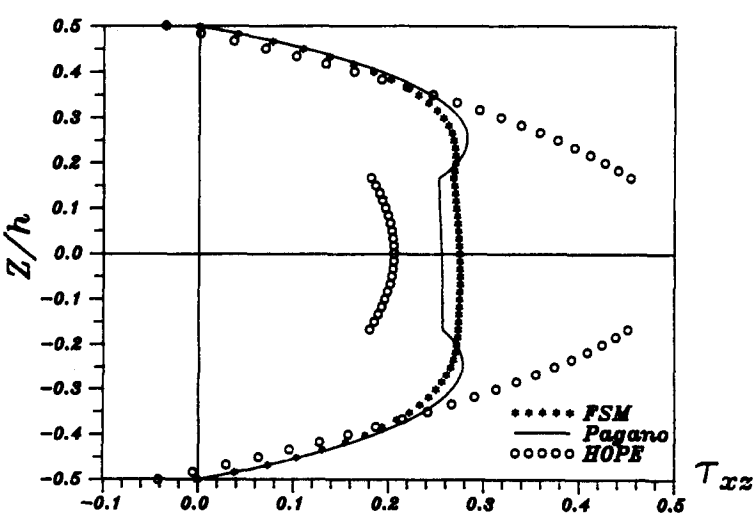

Fig. 9. Through-thickness distribution of transverse shear stress $\bar{\tau}_{xz}(0, a/2, z/h)$ for $a/h = 4$ three-layered plate.

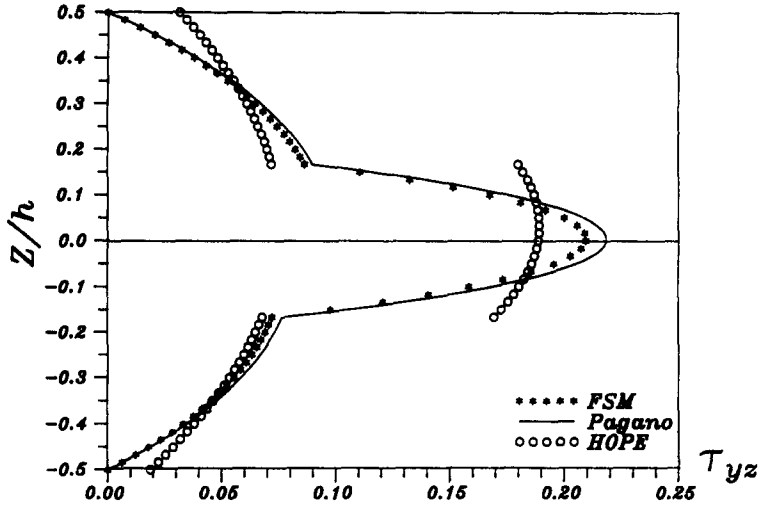

Fig. 10. Through-thickness distribution of transverse shear stress $\bar{\tau}_{yz}(a/2, 0, z/h)$ for $a/h = 4$ three-layered plate.

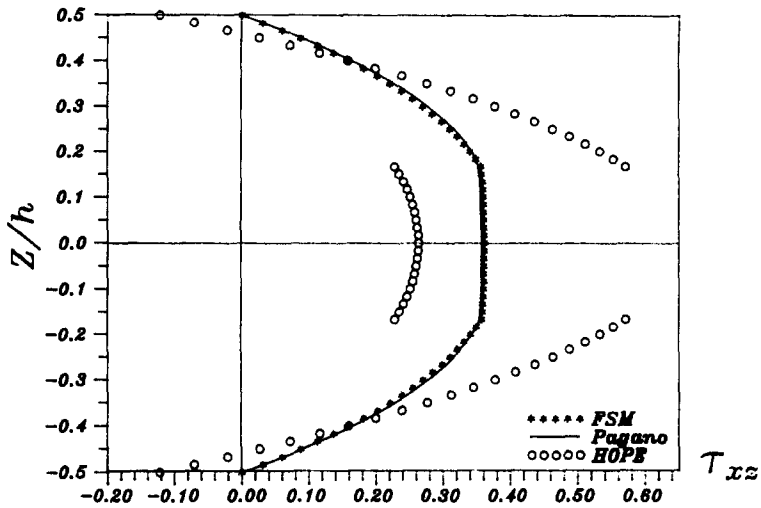

Fig. 11. Through-thickness distribution of transverse shear stress $\bar{\tau}_{xz}(0, a/2, z/h)$ for $a/h = 10$ three-layered plate.

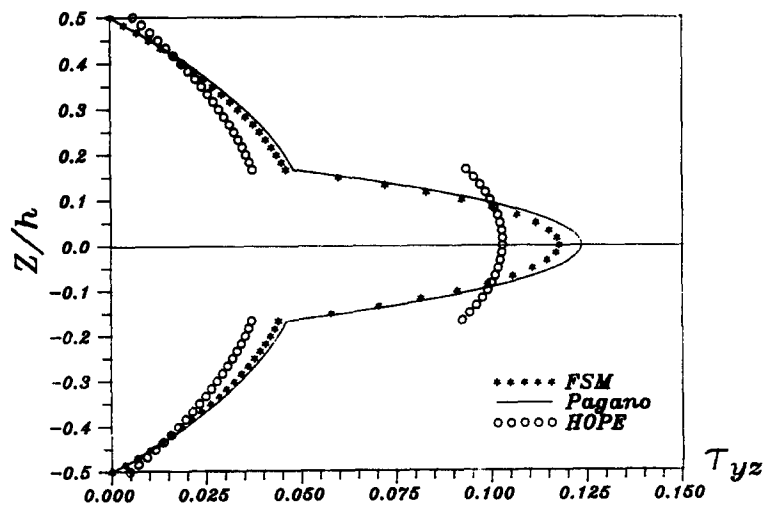

Fig. 12. Through-thickness distribution of transverse shear stress $\bar{\tau}_{yz}(a/2, 0, z/h)$ for $a/h = 10$ three-layered plate.

Table 5. Normalized transverse maximum deflection of three-layer, (0°/90°/0°) square plate under sinusoidal loading

	Deflection $\bar{w} = 100E_{22}w(a/2, a/2, 0)/q_0hS^4$		
	Present	Reddy	Pagano
$S = 4$	1.89855	1.9218	2.01420
$S = 10$	0.71511	0.7125	0.75300
$S = 20$	0.50557	0.4342	0.51978
$S = 50$	0.44329	—	0.44820
$S = 100$	0.43426	—	0.43777

Reddy (1984a): refined C^1 higher-order plate theory.

Table 6. Normalized transverse maximum deflection of three-layer, (0°/90°/0°) square plate under uniform loading

	Deflection $\bar{w} = 100E_{22}w(a/2, a/2, 0)/q_0hS^4$	
	Present	Reddy
$S = 4$	2.8760	2.9103
$S = 10$	1.0963	1.0903
$S = 20$	0.7790	0.7761
$S = 50$	0.6847	0.6839
$S = 100$	0.6700	0.6705

Reddy (1984b): refined C^1 higher-order plate theory.

The through-thickness distribution of $(\bar{\sigma}_x, \bar{\sigma}_y, \bar{\tau}_{xy}, \bar{\tau}_{yz})$ for the $S = 4$ laminate is depicted in Figs 5–8. FSM and HOPE both yield accurate flexural stresses. While the transverse shear stresses are calculated through the stress equilibrium equation, the predicted $\bar{\tau}_{yz}$ is in good agreement with the exact solution.

Three-layer composite laminate

Three-layer (0°/90°/0°) cross-ply simply-supported laminated square plates are studied. Sinusoidal loading and uniform loading are both investigated.

Table 5 tabulates the normalized centre deflection $\bar{w}$ for sinusoidally loaded laminates, and Table 6 is for uniformly loaded laminates. For the case of a sinusoidal loading, a three-dimensional elasticity solution is available. It is clear that the present results are better than the refined C^1 higher-order plate theory by Reddy (1984a) for $S = 4$ and 10 plates. Although there exists a strangely large error for the $S = 20$ plate in Reddy's solution, the error of the present model is only 2.73%. On the other hand, no elasticity solution is available for the case of uniform loading. The numerical results using three terms are close to the series solution by Reddy (1984b).

The through-thickness stress distribution is also exhibited for the case of a sinusoidal loading. Similarly, accurate flexural stresses are obtained in both FSM and HOPE. While the stress equilibrium equation is adopted, the distribution of $(\bar{\tau}_{xz}, \bar{\tau}_{yz})$ resembles the elasticity solution. They are plotted in Figs 9, 10 for the $S = 4$ plate, and in Figs 11, 12 for the $S = 10$ plate.

CONCLUSIONS

A refined finite strip method using the higher-order plate theory has been proposed in this paper. The comparative benchmark problems are given to demonstrate the adequacy and accuracy of the present study. The transverse shear deformation can be effectively evaluated, wherein the shear coefficient is not required. Meanwhile, the severe warping of the cross-section is also closely predicted. With far fewer degrees of freedom, the present model yields similar or even better results than the closed-form or finite element solutions. It is thought to be attributed to the fact that the eigenfunctions $Y_m(y)$ exactly satisfy the simply-supported boundary conditions. Owing to the accuracy shown in this study, the application of higher-order plate theory to the finite strip method for laminated plates with different support conditions or to the spline finite strip method can be executed with confidence.

REFERENCES

Cheung, M. S. and Cheung, Y. K. (1972). Static and dynamic behaviour of rectangular plates using higher finite strips. *Build. Sci.* **7**, 151–158.

Cheung, Y. K. (1976). *Finite Strip Method in Structure Analysis*. Pergamon Press, Oxford.

Kant, T. and Pandya, B. N. (1988). A simple finite element formulation of a higher-order theory for unsymmetrically laminated composite plates. *Compos. Struct.* **9**, 215–246.

Levinson, M. (1980). An accurate, simple theory of the statics and dynamics of elastic plates. *Mech. Res. Comm.* **7**, 343–350.

Lo, K. H., Christensen, R. M. and Wu, E. M. (1977). A higher-order theory of plate deformation. Part 2—Laminated plates. *J. Appl. Mech.* **44**, 669–676.

Mawenya, A. S. and Davies, J. D. (1974). Finite strip analysis of plate bending including transverse shear effects. *Build. Sci.* **9**, 175–180.

Pagano, N. J. (1969). Exact solutions for composite laminates in cylindrical bending. *J. Compos. Mater.* **3**, 398–411.

Reddy, J. N. (1984a). A simple higher-order theory for laminated composite plates. *J. Appl. Mech.* **51**, 745–752.

Reddy, J. N. (1984b). Energy and variational method in applied mechanics. Wiley-Interscience, Chichester.

Yang, H. Y. and Chong, K. P. (1984). Finite strip method with X-spline function. *Comput. Struct.* **18**, 127–132.